International Journal of Nanomedicine

Dovepress
open access to scientific and medical research

Open Access Full Text Article

ORIGINAL RESEARCH

The preosteoblast response of electrospinning PLGA/PCL nanofibers: effects of biomimetic architecture and collagen I

This article was published in the following Dove Press journal:
International Journal of Nanomedicine
25 August 2016
Number of times this article has been viewed

Yunzhu Qian[1,2]
Hanbang Chen[1]
Yang Xu[1]
Jianxin Yang[2]
Xuefeng Zhou[3]
Feimin Zhang[1]
Ning Gu[3]

[1]Jiangsu Key Laboratory of Oral Diseases, Nanjing Medical University, Nanjing, [2]Center of Stomatology, The Second Affiliated Hospital of Soochow University, Suzhou, [3]School of Biological Science and Medical Engineering, Southeast University, Nanjing, People's Republic of China

Abstract: Constructing biomimetic structure and incorporating bioactive molecules is an effective strategy to achieve a more favorable cell response. To explore the effect of electrospinning (ES) nanofibrous architecture and collagen I (COL I)-incorporated modification on tuning osteoblast response, a resorbable membrane composed of poly(lactic-co-glycolic acid)/poly(caprolactone) (PLGA/PCL; 7:3 w/w) was developed via ES. COL I was blended into PLGA/PCL solution to prepare composite ES membrane. Notably, relatively better cell response was delivered by the bioactive ES-based membrane which was fabricated by modification of 3,4-dihydroxyphenylalanine and COL I. After investigation by field emission scanning electron microscopy, Fourier transform infrared spectroscopy, contact angle measurement, and mechanical test, polyporous three-dimensional nanofibrous structure with low tensile force and the successful integration of COL I was obtained by the ES method. Compared with traditional PLGA/PCL membrane, the surface hydrophilicity of collagen-incorporated membranes was largely enhanced. The behavior of mouse preosteoblast MC3T3-E1 cell infiltration and proliferation on membranes was studied at 24 and 48 hours. The negative control was fabricated by solvent casting. Evaluation of cell adhesion and morphology demonstrated that all the ES membranes were more favorable for promoting the cell adhesion and spreading than the casting membrane. Cell Counting Kit-8 assays revealed that biomimetic architecture, surface topography, and bioactive properties of membranes were favorable for cell growth. Analysis of β1 integrin expression level by immunofluorescence indicated that such biomimetic architecture, especially COL I-grafted surface, plays a key role in cell adhesion and proliferation. The real-time polymerase chain reaction suggested that both surface topography and bioactive properties could facilitate the cell adhesion. The combined effect of biomimetic architecture with enhanced surface activity by 3,4-dihydroxyphenylalanine-assisted modification and COL I incorporation of PLGA/PCL electrospun membranes could successfully fill osteogenic defects and allow for better cell proliferation and differentiation.

Keywords: guided bone regeneration, biomimetic architecture, bioactive molecular, preosteoblast response, collagen

Introduction

The guided bone regeneration (GBR) technique is widely used to treat mandible and alveolar bone defects, and facilitate the natural biological potential by creating a favorable environment for peri-implant regeneration in dental implant and prosthetic dentistry.[1,2] GBR membrane acts as a barrier to prevent epithelial and connect tissue downgrowth into the defect. Hence, it protects and allows the healing process by maintenance of a space where cells from the surrounding bone tissue can migrate,

Correspondence: Feimin Zhang
Jiangsu Key Laboratory of Oral Diseases, Nanjing Medical University, Hanzhong Road, Nanjing 210029, People's Republic of China
Tel +86 138 0158 9779
Fax +86 25 8651 6414
Email fmzhang@njmu.edu.cn

submit your manuscript | www.dovepress.com
Dovepress
http://dx.doi.org/10.2147/IJN.S110577

stimulate in situ bone regeneration, and amplify alveolar ridge levels for implant stability.[3–6] The ideal GBR membrane for orthopedic tissue application should be biodegradable and biocompatible, as well as have a multiporous three-dimensional (3D) architecture favorable for cell attachment and differentiation.

The drawbacks of conventional membranes largely impede their clinical application. As previously reported, the non-resorbable membranes always accompany a secondary surgical procedure for removal and may lead to additional patient discomfort. Also, conventional collagen-based resorbable membranes result in the loss of space maintenance and are associated with a risk of disease transmission to human from animal-derived collagen. In recent years, the resorbable membranes based on poly(lactic acid), poly(lactic-co-glycolic acid) (PLGA), poly(caprolactone) (PCL), and their composites have attracted significant attention, due to their low rigidity, manageability, processability, tuned biodegradation, and drug-encapsulating ability.[7,8] Synthetic polymers PLGA and PCL are the important membranes in the family of the US Food and Drug Administration-approved aliphatic polyesters for their superior mechanical properties, spinnability, flexibility, biocompatibility, porosity, and controllable degradability.[9,10] Studies have shown that PLGA fibrous scaffolds are stiffer while PCL is more compliant in response to mechanical loading. Hence, PLGA/PCL hybrid membrane has combined the biological and mechanical advantages of both PLGA and PCL, which can be used as a desirable candidate for fabricating GBR membrane due to its selective permeability, flexibility, adhesiveness with bone, osteoconductivity, and excellent mechanical strengths (both tensile and suture pullout strengths).[11,12]

The goal of membrane/scaffold design for bone tissue engineering is to produce a biomaterial matrix that can replace the natural extracellular matrix (ECM), by which the seeded cells can produce a new natural matrix and regenerate the desired tissue structure. Critical parameters for designing membrane/scaffold in GBR technique include biocompatibility, biodegradability, optimal mechanical strength, and ability to regulate appropriate cellular activities.[13–15] An "ideal" degradable GBR polymeric membrane has yet to be found due to the disadvantage of polyester-based resorbable membranes (eg, poor cell response/weak osteoconductive or osteoinductive properties). To address this challenge, various approaches have been emerged to meet the demands of degradable GBR polymeric membranes in terms of mechanical properties, biocompatibility, and biological response, such as the following strategies:

1) Assembling multiple polymers (synthetic or natural) to maximize the advantages and minimize respective disadvantages.[9,16]
2) Designing 3D nano-scaffolds to mimic the ECM.[17]
3) Fabricating functionally graded and multilayered membranes.[18]
4) Incorporating osteoconductive calcium phosphate ceramics (eg, β-tricalcium phosphate, hydroxyapatite),[19,20] antibacterial agents (eg, metronidazole), bioactive proteins (eg, BMP-2), or growth factors (eg, stromal cell-derived factor-1α) into biodegradable polymers.[8,21]
5) Modifying the biomembrane surface to graft bioactive molecules or proteins (eg, 3,4-dihydroxyphenylalanine [pDA]).[22,23]

Due to biomimetic fabrication of GBR membrane, surface modification of the synthetic polymers is also considered a key factor in tissue engineering. By immobilizing bioactive molecules (eg, polypeptide[24,25] and collagen[26,27]), their interaction with cells can be greatly improved, along with the accelerated bone regeneration by inducing biological guidance. Collagen is a major constituent of natural ECM with excellent cell affinity and biocompatibility.[28] In recent years, collagen I (COL I) has been widely investigated and presents excellent properties that facilitate cell attachment as well as enhance surface bioactivity by modifying biomaterial surfaces.[29] However, the hybrid membrane with COL I coated onto the surface shows a rapid degradation rate, which exceeds the rate of bone regeneration. Similar to other adhesive peptides and growth factors, COL I is immobilized onto biomaterial surfaces via either chemical or physical strategies to avoid rapid degradation.[30] The important role of COL I in cell adhesion, proliferation, and bone mineralization is still far from being well understood.

Among the conventional fabrication techniques, electrospinning (ES) is a particularly promising technique used to fabricate tissue-engineered scaffolds comprising nonwoven, 3D, porous, and nanoscale fiber-based matrix for GBR application. In our study, a well-defined resorbable membrane composed of PLGA/PCL (7:3, w/w) with 3D nanofibrous scaffolds was established via sequential multilayer ES. COL I was blended with PLGA/PCL solution to prepare the composite ES membrane. The immobilization of pDA and polydopamine-modified COL I onto ES membranes was achieved, and the surface-modified bioactive ES membranes were obtained (Figure 1). Five different membranes were prepared for culturing mouse preosteoblast MC3T3-E1 cells in vitro, and the effects of biomimetic architecture, surface topography, and bioactive properties on cell adhesion and

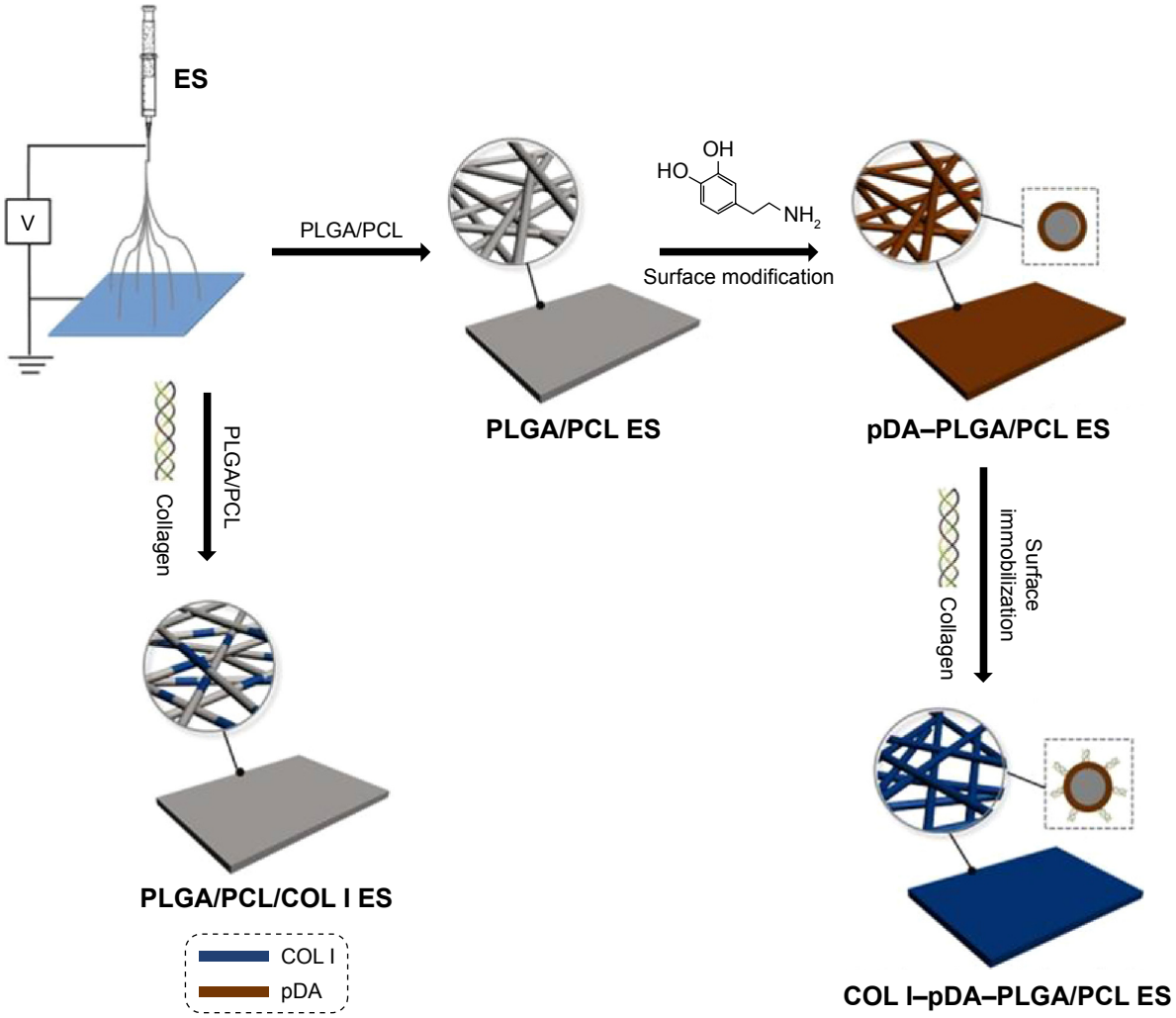

Figure 1 Schematic illustration of fabricating PLGA/PCL electrospun membranes.
Note: The schematic representation of fabricating the ES membranes: PLGA/PCL ES; pDA–PLGA/PCL ES; PLGA/PCL/COL I ES; and COL I–pDA–PLGA/PCL ES.
Abbreviations: PLGA, poly(lactic-co-glycolic acid); PCL, poly(caprolactone); ES, electrospinning; pDA, 3,4-dihydroxyphenylalanine; COL I, collagen I.

proliferation were investigated. The expression of β1 integrin specific to osteoblast was evaluated. As collagen is a main component of bone and cartilage ECM, we hypothesized that the combined effect of biomimetic architecture and bioactivity by COL I could enhance osteoconductive behavior of PLGA/PCL electrospun membranes.

Materials and methods

Materials

PLGA (75:25, M_W =120,000 Da) and PCL (M_W =80,000 Da) were purchased from Jinan Daigang Biomaterials (Jinan, People's Republic of China). COL I (rat tail collagen) was obtained from Thermo Fisher Scientific (Waltham, MA, USA). Dopamine hydrochloride was acquired from Sigma-Aldrich Co. (St Louis, MO, USA). 2,2,2-Trifluoroethanol (99.5%) was purchased from Aladdin (Shanghai, People's Republic of China). Tris–HCl solution (pH 8.5) was purchased from Beyotime (Shanghai, People's Republic of China). α-Modified minimum essential medium (1X), fetal bovine serum, penicillin–streptomycin solution, and 0.25% trypsin (1X) solution were purchased from HyClone (Logan, UT, USA). (4-(2-Hydroxyethyl)-1-piperazineethanesulfonic acid) buffer solution was purchased from Sigma-Aldrich Co. Rhodamine phalloidin was purchased from Cytoskeleton, Inc. (Denver, CO, USA). 4′,6-Diamidino-2-phenylindole was purchased from Beyotime. Albumin bovine (from bovine serum) was purchased from Solarbio (Beijing, People's Republic of China). PrimeScript RT reagent kit was obtained from Shengong (Shanghai, People's Republic of China). Anti-β1 integrin was purchased from Abcam plc (Cambridge, UK). Fluorescein isothiocyanate goat anti-rabbit IgG (H+L) antibody was purchased from Abalone (FR, Hangzhou,

People's Republic of China). Ultrapure water was prepared by using a Milli-Q water purification system (EMD Millipore, Billerica, MA, USA).

Preparation of five different PLGA/PCL membranes

Five membrane samples (PLGA/PCL ES, PLGA/PCL ES membranes; PLGA/PCL, membranes fabricated by solvent casting; PLGA/PCL/COL I ES, COL I was blended into PLGA/PCL solution to prepare the composite ES membrane; pDA–PLGA/PCL ES, PLGA/PCL ES membrane with pDA coating only; COL I–pDA–PLGA/PCL ES, COL I immobilized onto ES membranes assisted by pDA) were prepared.

All membranes were prepared by a polymer blend composed of (7:3, w/w) PLGA and PCL. For PLGA/PCL solution, PLGA 0.7 g and PCL 0.3 g were, respectively, dissolved in 7.3 g 2,2,2-trifluoroethanol and stirred overnight. For ES, 4 mL PLGA/PCL solution was placed in a 10 mL glass syringe fit with a 6# needle (Ling Pai, Shanghai, People's Republic of China) and placed in a syringe pump (Zhejiang Smith Medical, Zhejiang, People's Republic of China). The collector was grounded to obtain a flat tip. The feeding rate of the pump was 0.6 mL h^{-1}. The fibers were fabricated by ES at an applied voltage of 16 kV using a high-voltage power supply (Dong Wen, Tianjin, People's Republic of China), and the tip-to-collector distance was 13–18 cm. Processing variables, including solution concentration, field strength (voltage), spinneret-to-collector distance, and flow rate, were optimized for this hybrid polymer system to obtain bead-free fibrous structures. For PLGA/PCL/COL I ES membrane, 250 μL COL I was added into the prepared PLGA/PCL solution with stirring for 5 hours by ES. For solvent casting, 4 mL PLGA/PCL solution was placed in a Petri dish at room temperature for 5 hours before standing for film.

As for the surface-modified bioactive ES membrane, pDA coating was performed as previously described.[31] These membranes were immersed into the alkaline polydopamine solution (2 mg/mL dissolved in the 10 mM Tris–HCl buffer solution, pH 8.5) and placed on a shaker for 24 hours at 25°C. This simple dip-coating was used to form a self-assembled pDA thin film on the surface of the PLGA/PCL ES membranes. During the self-polymerization of pDA, the change in color from light brown to black was observed. The pDA-coated membranes were then rinsed with deionized water gently to remove unattached pDA molecules. Then, the pDA-coated ES membranes were soaked into 2% glutaraldehyde water solution (prepared from 25% glutaraldehyde water solution; Hushi, Suzhou, People's Republic of China) for 1 hour. After being rinsed with deionized water gently for at least three times, the membranes were incubated in 12.5 μL/mL COL I solution (250 μL COL I dissolved in the 20 mL sterile phosphate-buffered saline [PBS] solution) for 24 hours. After rinsing as described, the COL I–pDA–PLGA/PCL ES membranes were prepared.

The membranes were dried for 24 hours in a vacuum oven at room temperature. All procedures were performed under aseptic conditions, and the prepared membranes were sterilized under UV for 4 hours before cell seeding.

Material characterization

Surface characterization

Microstructures of the samples were observed by field emission scanning electron microscopy (SEM; JSM-7401F; JEOL, Tokyo, Japan). Each sample was kept for 48 hours at room temperature in a vacuum desiccator to remove any residual solvent. Surface functional groups were evaluated by performing attenuated total reflectance infrared spectroscopy on a Fourier transform infrared (FTIR) spectrophotometer (Nicolet 6700; Thermo Fisher Scientific), coupled with Omni-ATR accessory, at a resolution of 4 cm^{-1} for 32 scans. The hydrophilic properties of the samples were investigated using a contact angle meter (SL200B; Solon [Shanghai] Technology Science, Shanghai, People's Republic of China). The diameter of droplet used for the measurement was ~2 mm. Ultrapure water droplets were placed at six different positions for one sample. The results were statistically analyzed.

Tensile property

Samples were cut into a rectangular shape, 10 mm in width and 20 mm in length. The thickness was measured by a Vernier caliper. Four random points on each membrane were measured, and the average was used as the thickness (~0.15 mm). The tensile strength and modulus of elasticity of the obtained samples were examined with an electronic universal testing machine (INSTRON 3365; INSTRON, Norwood, MA, USA). Sand paper was used to clamp both ends of the samples to prevent slipping during the testing. The crosshead speed was set at 1 mm/min. The yield point value of the stress–strain curve was determined as the tensile strength, and the elasticity modulus was calculated by the slope of the linear portion of the curve.

In vitro cell activity tests

For cell proliferation, pure cell culture without membrane was used as the blank control. For cell attachment and β1 integrin immunofluorescence, untreated coverslip with cell culture was used as the blank control, and the rough surface of natural

collagen (I and III) membrane (Geistlich Bio-Gide® 13×25 mm; Geistlich Pharma AG, Wolhusen, Switzerland) was used as the positive control. The MC3T3-E1 cell line (subclone 14) was purchased from the Cell Bank of the Chinese Academy of Sciences (Shanghai, People's Republic of China). Cells were cultured in a complete medium containing α-modified minimum essential medium (HyClone) supplemented with 10% fetal bovine serum (HyClone), 100 mg/mL streptomycin, and 100 U/mL penicillin (Beyotime). After reaching 80%–90% confluence, the cells were detached using 0.25% trypsin (Thermo Fisher Scientific) containing ethylenediaminetetraacetic acid and counted with a hemocytometer. Cells were subcultured at least twice a week and were maintained at a humidified atmosphere of 95% air and 5% CO_2. Cells below passage 10 were used for this study.

Sample preculture

Before cell seeding, five well-prepared samples were placed in a 96-well plate in a complete medium described earlier and precultured in an incubator (37°C, 5% CO_2) for 24 hours. After removing culture solution, samples were ready for subsequent use.

Cell proliferation

The cell proliferation was investigated by a Cell Counting Kit-8 (CCK-8; Beyotime) assay. Cells were plated in a 96-well plate at a density of 2×10^3 cells/well in triplicate. At 1, 3, 5, and 7 days after seeding, the cell viability was measured using CCK-8 assays according to the manufacturers' instructions. The optical density (OD) at 450 nm was determined via an enzyme-linked immunosorbent assay plate reader (Titertek-Berthold, Huntsville, AL, USA). Three independent experiments were performed for each assay condition.

Cell attachment

The morphology of cells that adhered to the surfaces was visualized after cultivation for 24 and 48 hours using confocal laser scanning microscopy (CLSM; Zeiss-LSM710; Carl Zeiss Meditec AG, Jena, Germany). The cells were seeded in a 24-well plate at a density of 1×10^4 cells/well in triplicate. For CLSM, the samples were washed with PBS (1X), fixed with 3.7% paraformaldehyde for 30 minutes at room temperature, and then permeabilized with 0.25% Triton X-100/PBS for 3 minutes. Cells were then incubated with rhodamine phalloidin (1:200 dilution; Cytoskeleton, Inc.) for 30 minutes and rinsed six times with PBS (1X). After incubation with 4′,6-diamidino-2-phenylindole (Beyotime) (1:2,000 dilution) for 30 seconds in the dark at room temperature, samples were rinsed three times with PBS (1X) and observed by CLSM.

β1 integrin immunofluorescence

After cultivation for 24 hours, the samples were rinsed with PBS (1X), fixed with 3.7% paraformaldehyde for 15 minutes at room temperature, permeabilized with 0.5% Triton X-100 in PBS for 3 minutes, and sequentially blocked with 3% bovine serum albumin for 30 minutes. Following overnight incubation with the specific primary detection antibody (β1; Abcam plc) (1:50 dilution), cells were further incubated with the secondary antibody, Alexa Fluor 488 goat antirabbit IgG (Beyotime) (1:200 dilution), and actin cytoskeleton staining was performed. Images were captured and analyzed using CLSM (Zeiss-LSM710).

RNA isolation and RT-PCR

The RNA isolation was performed by collecting the cells and extracting the RNA using the TRIzol reagent (Thermo Fisher Scientific). The corresponding reverse transcription reactions were performed by the PrimeScript RT reagent kit (Shengong). Real-time polymerase chain reactions (RT-PCRs) were performed using the SYBR Premix Ex Taq kit (TaKaRa Bio Co., Ltd., Otsu, Japan) with the generated cDNA as the template; the corresponding sequences of primers used in this study are listed in Table 1. For the RT-PCRs, the ABI 7300 Real-time PCR System (Applied Biosytems, Foster City, CA, USA) was used with the following conditions: 95°C for 5 minutes, followed by 40 cycles of amplification, 95°C for 10 seconds for the denaturation reaction, and an extension step at 60°C for 31 seconds. The expression level of target gene was normalized to glyceraldehyde-3-phosphate dehydrogenase, and the relative gene expression values were calculated by the $2^{-\Delta\Delta Ct}$ method.

Statistical analysis

Statistical analysis was performed by the SPSS v.19.0 software (IBM Corporation, Armonk, NY, USA). Data are

Table 1 Primers for real-time polymerase chain reaction analysis

Gene	Forward primer (5′–3′)	Reverse primer (5′–3′)
β1 integrin	ATCCCAATTGTAGCAGGCGTGGTT	GACCACAGTTGTCACGGCACTC

presented as the mean ± standard deviation. Significance was accepted at a level of $P<0.05$. After testing the normality, statistical analysis was performed using one-way analysis of variance followed by the least significant difference test. All quantitative data reported represent the mean of at least three independent experiments.

Results and discussion

Microstructure of membranes

Field emission SEM images of five different membranes are shown in Figure 2: PLGA/PCL ES (Figure 2A), PLGA/PCL (Figure 2B), PLGA/PCL/COL I ES (Figure 2C), pDA–PLGA/PCL ES (Figure 2D), and COL I–pDA–PLGA/PCL ES (Figure 2E). The fiber characteristics (diameter, porosity, etc) and structure morphology depend on the process parameters (high voltage, feed rate, etc) and polymer solution characteristics (viscosity, conductivity, etc). To achieve favorable mechanical properties, PLGA/PCL nanofibrous scaffolds were electrospunned in a tunable and predictable manner for providing a suitable ECM-like environment.

Uniform and compact PLGA/PCL ES fibers (average fiber diameter, 860.6±213.0 nm) were randomly arranged, forming rough surfaces. Three-dimensional, interconnected pores between the fibers were distributed throughout the scaffold matrix (Figure 2A). PLGA/PCL/COL I ES membranes (average fiber diameter, 827.2±191.0 nm) showed the similar 3D topography as PLGA/PCL ES, while the topographies of PLGA/PCL membranes prepared by solvent casting were planar structured. The micropores in the relatively smooth membranes varied significantly not only in number but also in size. The surface morphology and fiber roughness of PLGA/PCL ES membranes were altered after pDA coating or pDA-mediated COL I immobilization (Figure 2D and E). SEM analysis demonstrated that PLGA/PCL nanofibers that underwent surface modification showed a rough surface morphology compared with unmodified ones. Deposition of the pDA layer and self-polymerized pDA particulates was observed on the surface of nanofibers indicating that the coating of the pDA layer increased the surface roughness of PLGA/PCL ES membranes. This result suggests that pDA coating can change the surface properties of polymer substrates. Immobilization of COL I increased the size of pDA particulates and surface roughness of the pDA–PLGA/PCL ES membranes. COL I–pDA–PLGA/PCL ES membranes with spider web-like topography penetrated into the interconnected scaffold pores. Among the most promising biomimetic materials, electrospun polymeric nanofibers can provide topographical and biochemical cues that resemble ECM and constitute aligned architectures to guide cell growth and spreading.[32]

Surface properties of PLGA/PCL ES membranes modified by pDA or pDA-assisted immobilization may affect cell proliferation and viability. With increased surface roughness, pDA–PLGA/PCL ES and COL I–pDA–PLGA/PCL ES membranes might be able to enable topographical stimulation that can facilitate focal adhesion formation in the cells.[33,34] This is attributed to the topographical stimulation induced by increased surface roughness. The change of rough surface may activate intracellular signal transductions for cell proliferation via enhanced focal adhesion formation, which are regulated by the actin cytoskeleton in a process that may involve integrin-mediated matrix binding and signaling pathways.[35,36]

Surface chemical characteristics

The FTIR spectra of PLGA/PCL ES, PLGA/PCL, PLGA/PCL/COL I ES, pDA–PLGA/PCL ES, and COL I–pDA–PLGA/PCL ES membranes are presented in Figure 3. There were two characteristic absorption bands at 1,756.4 and 1,725.3 cm^{-1} attributed to the free ester groups in the pristine PLGA and conjugated ester groups in PCL, respectively.[37,38] The spectrum also showed strong bands near 1,186.1 and 1,092.4 cm^{-1} due to a C–O–C group in the structure. The multiple absorption peaks at 1,240–961 cm^{-1} were assigned to C–O–C vibration mode. The peaks at 2,945.6 and 2,866.8 cm^{-1} were assigned to stretching vibration of C–H in benzene methyl and methylene groups, respectively.[39] The absorption band of PLGA/PCL was similar to the PLGA/PCL ES except the strength. When the collagen was added, the typical bands of collagen were not found due to lower concentrations of collagen. However the peak strength of spectra of the free ester groups in the pristine PLGA and conjugated ester groups in PCL changed. It indicated that the surface composition had changed. After the introduction of pDA, the corresponding conspicuous peaks of pDA–PLGA/PCL ES appeared at 3,000 to 3,400 cm^{-1} which were attributed to the NH stretching and the OH stretching, respectively. The peak strength of methyl and methylene groups was decreased, respectively. For the FTIR spectra of COL I–pDA–PLGA/PCL ES, a band attributed to the C=O stretching vibration at 1,653.2 cm^{-1} and a band to N–H bending at 1,557.9 cm^{-1} for amide were seen.[40] This result suggested that the collagen was grafted on the pDA–PLGA/PCL ES surface. A group of samples with different bioactivities were carefully designed by the blend modification and pDA-mediated surface modification.

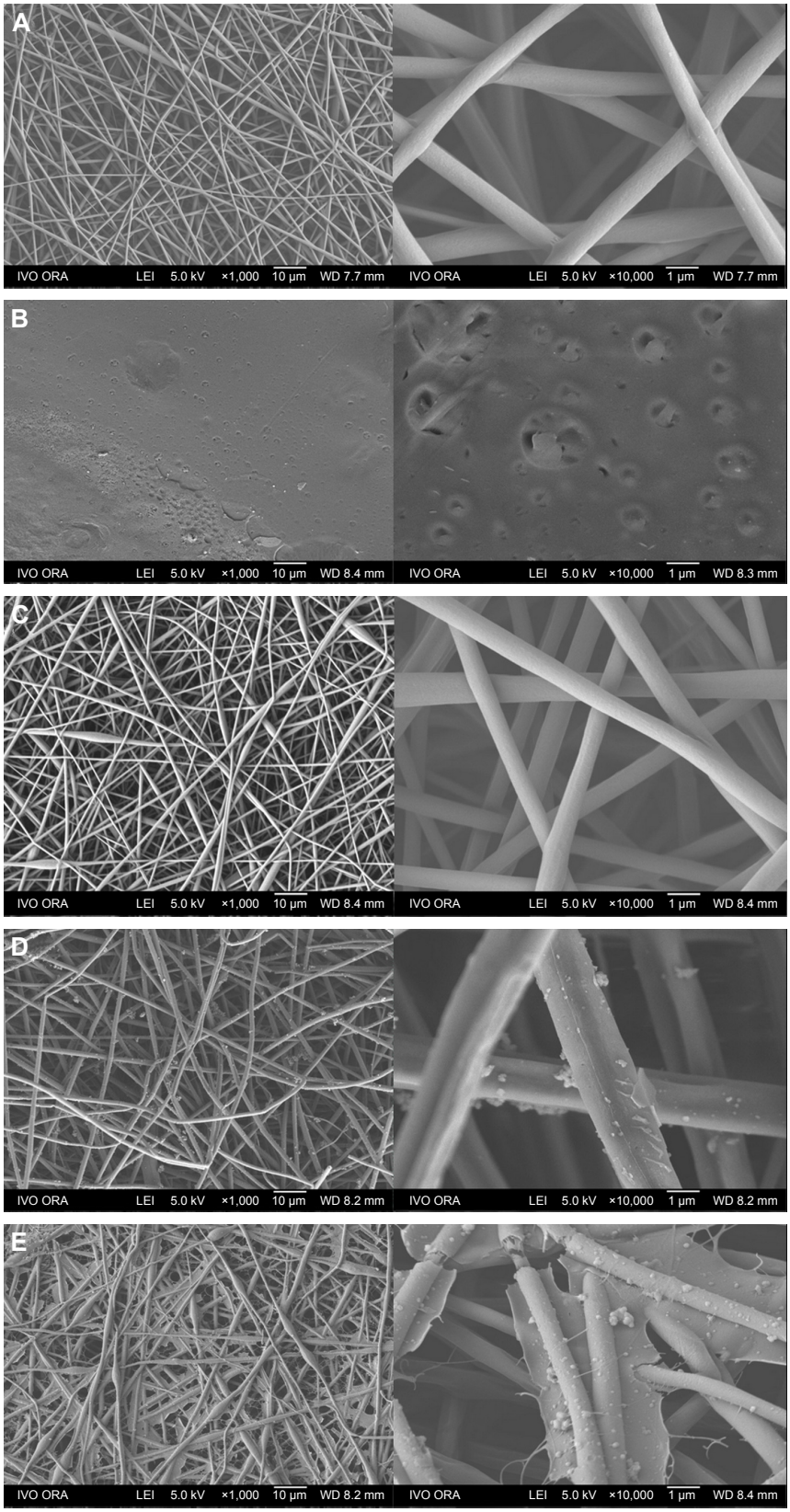

Figure 2 FE-SEM images of PLGA/PCL membranes.
Notes: (**A**) PLGA/PCL ES (ES parameters 20 kV, 18 cm, and 0.6 mL h^{-1}). (**B**) PLGA/PCL. (**C**) PLGA/PCL/COL I ES. (**D**) pDA–PLGA/PCL ES. (**E**) COL I–pDA–PLGA/PCL ES. Magnification of images on the left: ×1,000; right: ×10,000.
Abbreviations: FE-SEM, field emission scanning electron microscopy; PLGA, poly(lactic-co-glycolic acid); PCL, poly(caprolactone); ES, electrospinning; COL I, collagen I; pDA, 3,4-dihydroxyphenylalanine.

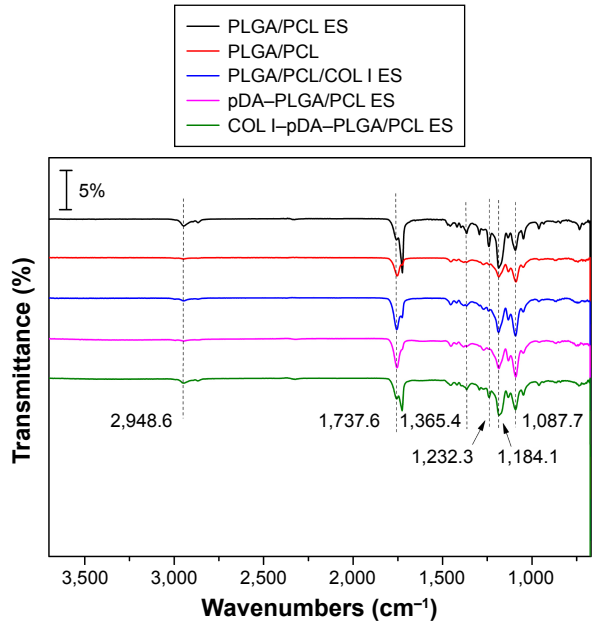

Figure 3 ATR-FTIR spectra of PLGA/PCL ES, PLGA/PCL, PLGA/PCL/COL I ES, pDA–PLGA/PCL ES, and COL I–pDA–PLGA/PCL ES membrane.
Abbreviations: ATR-FTIR, attenuated total reflectance-Fourier transform infrared; PLGA, poly(lactic-co-glycolic acid); PCL, poly(caprolactone); ES, electrospinning; COL I, collagen I; pDA, 3,4-dihydroxyphenylalanine.

Hydrophilic properties

The water contact angle of the five different membranes was measured in order to analyze the change in wettability of the polymer surface and is displayed in Figure 4. PLGA/PCL membranes indicated favorable hydrophilicity by solvent casting and typically exhibited a water contact angle of 65.0°±5.6°. PLGA/PCL ES membranes as well as PLGA/PCL/COL I ES membranes obtained by ES, in the 3D nanofibrous architecture with interconnected pores full of air, propped up the drops deposited on the surface with the biggest contact angles at 120.9°±10.1° and 126.8°±1.5°, respectively. The pDA coating rendered PLGA/PCL ES surfaces more hydrophilic, which was indicated by a decrease in contact angle from a starting angle of 120.9°±10.1° (PLGA/PCL ES) to 98.9°±8.4° (pDA–PLGA/PCL ES). In a previous study, the contact angle of PLGA thin film, a similar hydrophilic surface, decreased after pDA functionalization from a starting angle of 68.6°±3.8° to 27.3°±6.8°, indicating that the polymer surface is proved to be more hydrophilic after pDA coating.[41] Furthermore, attributed to the achieved modification of COL I with superior hydrophilicity mediated by pDA coatings onto the surface of PLGA/PCL interconnected nanofibers, the contact angle of COL I–pDA–PLGA/PCL ES dramatically descended to 5.0°±1.2°. There was a significant difference in hydrophilicity in the PLGA/PCL ES membrane before and after modification by pDA coatings ($P<0.05$) or immobilization of bioactive molecules mediated by pDA coatings ($P<0.05$), which may provide the more appropriate surface wettability for attachment and proliferation of cells such as endothelial cells, neural stem cells (NSCs), and mesenchymal stem cells (MSCs) reported in several studies.[37,42] The results were consistent with the results of FTIR, and indicated that the immobilization of pDA and COL I on PLGA/PCL ES was achieved.

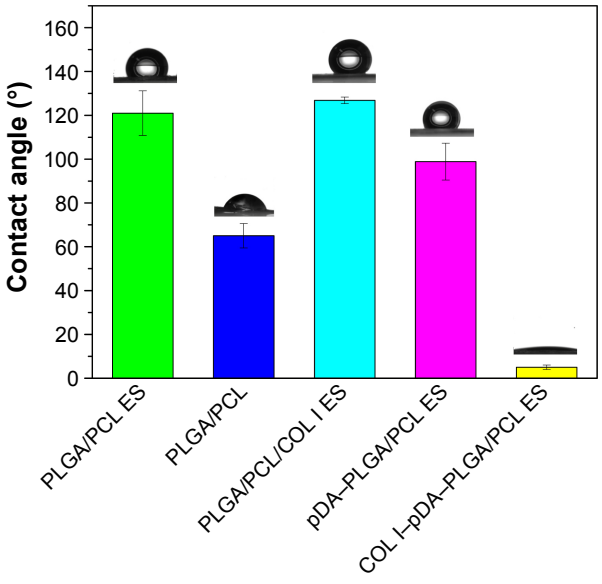

Figure 4 The water contact angle of PLGA/PCL ES, PLGA/PCL, PLGA/PCL/COL I ES, pDA–PLGA/PCL ES, and COL I–pDA–PLGA/PCL ES membranes.
Note: There was statistically significant difference between the contact angle of COL I–pDA–PLGA/PCL ES and that of the other four samples ($P<0.05$).
Abbreviations: PLGA, poly(lactic-co-glycolic acid); PCL, poly(caprolactone); ES, electrospinning; COL I, collagen I; pDA, 3,4-dihydroxyphenylalanine.

Mechanical properties

The mechanical properties of the five different membranes are shown in Figure 5. The PLGA/PCL membranes fabricated by solvent casting exhibited high elasticity modulus and tensile strength of 305.33±65.06 and 3.48±0.16 MPa, respectively. There was a significant difference in elasticity modulus and tensile strength between the PLGA/PCL membranes fabricated by solvent casting and the other four groups (n=4, $P<0.05$). No significant difference was found in elasticity modulus and tensile strength between the PLGA/PCL ES membranes and PLGA/PCL/COL I ES membranes (n=4, $P<0.05$), indicating that addition of a small amount of collagen may not significantly change the mechanical properties of the PLGA/PCL ES membranes. After modification by pDA coatings ($P<0.05$) or immobilization of bioactive molecules mediated by pDA coatings ($P<0.05$), the elasticity modulus of the PLGA/PCL ES membranes significantly increased, while there was no significant difference in the

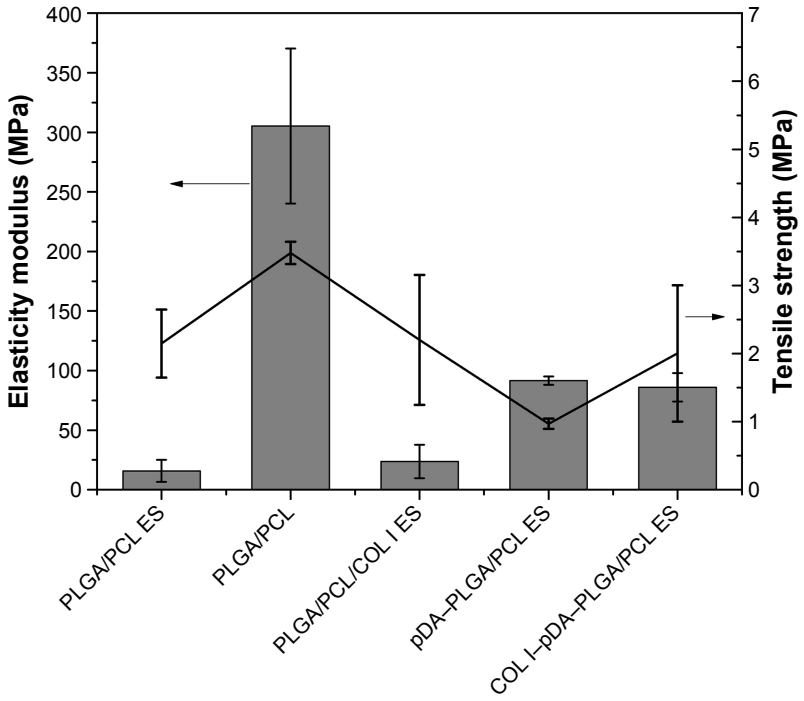

Figure 5 The mechanical properties of PLGA/PCL ES, PLGA/PCL, PLGA/PCL/COL I ES, pDA–PLGA/PCL ES, and COL I–pDA–PLGA/PCL ES membranes.
Note: There was a significant difference in both elasticity modulus and tensile strength between the PLGA/PCL membranes fabricated by solvent casting and the other four groups (n=4, $P<0.05$).
Abbreviations: PLGA, poly(lactic-co-glycolic acid); PCL, poly(caprolactone); ES, electrospinning; COL I, collagen I; pDA, 3,4-dihydroxyphenylalanine.

elasticity modulus between the pDA–PLGA/PCL ES and COL I–pDA–PLGA/PCL ES membranes (n=4, $P>0.05$). Therefore, COL I–pDA–PLGA/PCL ES membranes with interconnected pore networks may exhibit better mechanical function and better biological performance.[20]

PLGA/PCL ES nanofibrous membranes and 3D cell culture

The five different membranes in research on which MC3T3-E1 cells were cultured for 12 hours successfully displayed different colors under CLSM by special fluorescent dyes. Electrospun nanofibers were 3D interconnected and are demonstrated in Figure 6A, C, D, and E with elongated pseudopodia from MC3T3-E1 cells stretching and penetrating in. In a 3D nanofibrous architecture, cells adhered and proliferated. Only flat growth was observed in the other three groups (Figure 6B, F, and G) despite the existence of elongated pseudopodia. Good cell adherence on the electrospun nanofibers might be due to the large surface area available for cell attachment. Cells were attached to the surfaces by discrete filopodia and exhibited long and numerous microvilli on their surfaces. It was interesting to see that microvilli of cells tended to attach to and grow along the polymer nanofibers whose diameter was similar to that of microvilli. The images of pDA–PLGA/PCL ES, COL I–pDA–PLGA/PCL ES, and Bio-Gide Collagen membranes showed that more cells adhered and proliferated, which indicated that bioactive molecules and a rough surface play an important role in directing cell behavior. Moreover, these electrospun hybrid collagen/PCL or collagen/PLGA scaffolds have been shown to support cell adhesion, assist cell infiltration, enhance cell proliferation, stimulate cell growth and differentiation in vitro, induce vascular formation, and maintain structural integrity in vivo.[43,44]

Cell attachment analysis

At 24 and 48 hours after seeding (Figure 7), live cells on the nanofibrous membrane appeared to be substantially more than those on the cast film, and exhibited a distribution of higher uniformity in accord with the 3D electrospun nanofibrous architecture. Cellular compatibility was accomplished by culturing mouse preosteoblast MC3T3-E1 cells on nanofibrous membranes in cell culture medium. These results were then confirmed by the CCK-8 assay. The cellular adhesion process is adjusted by the interaction of the cell with the ECM, resulting in the formation of focal adhesions and organization of the cytoskeleton. Rather than direct contact with the material, cells interact with the adsorbed protein layer on the surface of the nanocomposites, which mediates the cell adhesion and provides signals to the cell through the

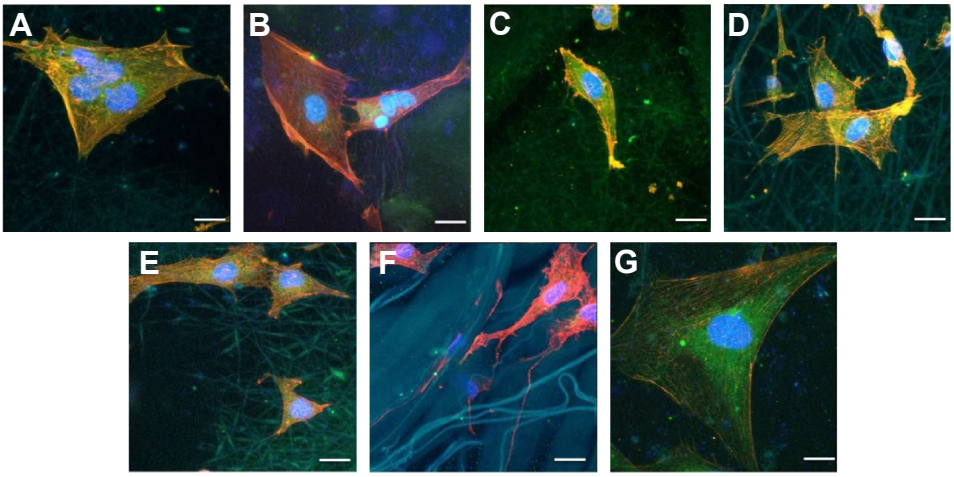

Figure 6 CLSM (×400) of morphology of cells cultured on five different membranes compared with untreated coverslips and Bio-Gide Collagen membranes.
Notes: (**A**) PLGA/PCL ES. (**B**) PLGA/PCL. (**C**) PLGA/PCL/COL I ES. (**D**) pDA–PLGA/PCL ES. (**E**) COL I–pDA–PLGA/PCL ES. (**F**) Bio-Gide Collagen membranes. (**G**) Untreated coverslips. Scale bars =20 μm. Cells were stained for F-actin (red), nucleus (blue), and substrates (green) by fluorescent dyes. Cell adhesion on the five different membranes was demonstrated by cellular morphology at 12 hours after seeding onto the membranes compared to untreated coverslips and Bio-Gide Collagen membranes.
Abbreviations: CLSM, confocal laser scanning microscopy; PLGA, poly(lactic-co-glycolic acid); PCL, poly(caprolactone); ES, electrospinning; COL I, collagen I; pDA, 3,4-dihydroxyphenylalanine.

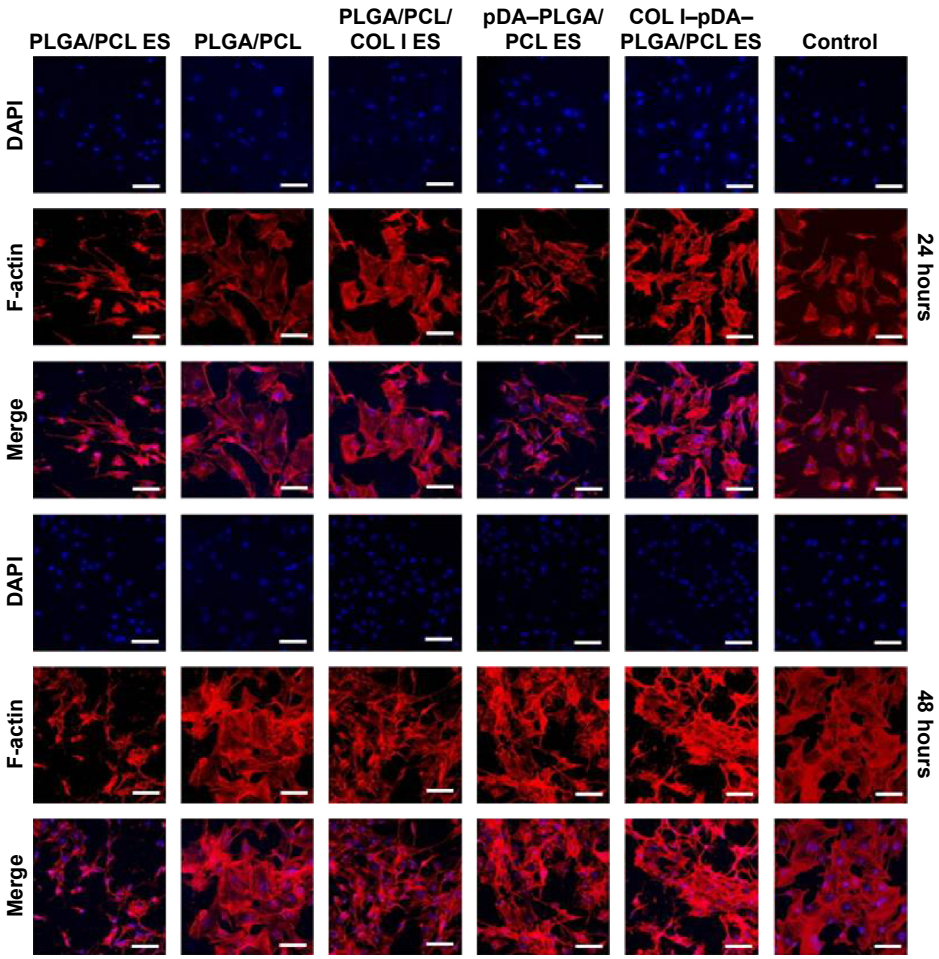

Figure 7 CLSM (×200) of morphology of cells cultured on five different membranes (PLGA/PCL ES, PLGA/PCL, PLGA/PCL/COL I ES, pDA–PLGA/PCL ES, COL I–pDA–PLGA/PCL ES) compared with untreated coverslips (blank control).
Notes: Cells were immunostained for F-actin (red) and nucleus (blue). Cell adhesion on different surfaces was compared by cellular morphology at 24 and 48 hours after seeding onto the six different surfaces. Scale bars =40 μm.
Abbreviations: CLSM, confocal laser scanning microscopy; PLGA, poly(lactic-co-glycolic acid); PCL, poly(caprolactone); ES, electrospinning; COL I, collagen I; pDA, 3,4-dihydroxyphenylalanine; DAPI, 4′,6-diamidino-2-phenylindole.

cell adhesion receptors – mainly integrins. The tripeptide amino acid sequence arginine–glycine–aspartic acid (RGD) is the minimal cell recognizable sequence present in many ECM and blood proteins such as fibronectin, vitronectin, and the collagens. RGD actively promotes cellular adhesion through binding to integrin receptors. As reported before, the cell–material interaction was enhanced by grafting the bioactive cell adhesion proteins or peptide motifs found in ECM molecules to the surface of the polymer membranes such as COL I and RGD peptides.[45] Our previous work suggested that topography of the surface as well as bioactive molecules (eg, collagen) plays an important role in the early stages of cell adhesion.[46] Moreover, the combined effects of the two types of properties provided an advantage in cell adhesion and spreading, possibly because of enhanced protein adsorption induced by the increased roughness or specific surface area. In our study, the electrospun nanofibrous architecture might be favorable for the mouse preosteoblast MC3T3-E1 cells for osteoconduction and as a source of osteogenic and osteoinductive substances for new bone formation.

Cell proliferation analysis

After cells adhere to the membranes, a series of processes including proliferation, differentiation, and ECM deposition continue to occur. Cell proliferation on the five different membranes was analyzed by CCK-8 assay at least three times compared with purely cultured MC3T3-E1 cells in vitro (Figure 8). Based on the absorbable PLGA/PCL, either electrospun or solvent-casted, and then COL I mixed for ES or COL I immobilized to ES membrane by pDA coating, increasing OD levels were observed from 1 to 7 days in all groups, indicating that the selected membrane substrate PLGA/PCL showed a considerable biocompatibility for cell proliferation. Although a significant difference between groups was, respectively, detected at 1, 3, and 5 days ($P<0.05$), there was no statistical difference between the five different membranes with the purely cultured cells ($P>0.05$) (Figure 8). When cultured for 1, 3, 5 days, the OD evaluated by the CCK-8 assay of the MC3TC-E1 cells cultured in the fabricated ES membranes has shown that the COL I-pDA-PLGA/PCL ES and the pDA-PLGA/PCL ES membranes were inferior for cell proliferation compared to the other four groups. However, cultured in the COL I-pDA-PLGA/PCL ES for 7 days, the OD of the cells has reached the highest; and the OD of the cells cultured in the pDA-PLGA/PCL ES for 7 days is higher than the PLGA/PCL ES, PLGA/PCL, and PLGA/PCL/COL I ES groups. pDA coating facilitates highly efficient, simple immobilization of neurotrophic growth factors and adhesion peptides onto polymer substrates

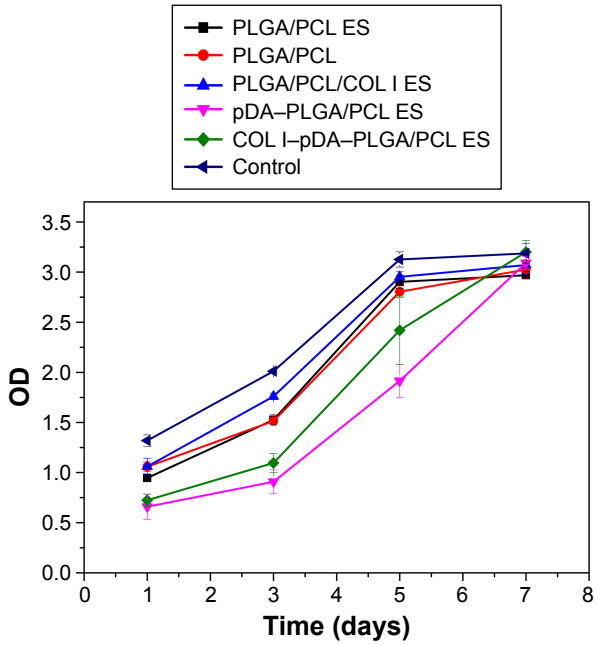

Figure 8 Proliferation of cells seeded on different PLGA/PCL membranes measured using CCK-8 assays (1, 3, and 5 days, n =3, $P<0.05$; 7 days, n=3, $P>0.05$; one-way ANOVA in SPSS v19.0).
Abbreviations: PLGA, poly(lactic-co-glycolic acid); PCL, poly(caprolactone); CCK-8, Cell Counting Kit-8; ANOVA, analysis of variance; OD, optical density; ES, electrospinning; COL I, collagen I; pDA, 3,4-dihydroxyphenylalanine.

which greatly enhance differentiation and proliferation of human NSCs at a comparable level. The pDA coating alone on PLGA substrates may enhance neuronal differentiation of human NSCs.[41] ECM proteins serve as nonsoluble cues to modulate cell fate through cell signaling cascades. COL I and fibronectin stimulate migration and proliferation of osteoblasts by direct binding to cellular transmembrane receptors. Combined with anionically charged polymers such as PLGA and polyvinylpyrrolidone-I, these collagen-based matrices promote osteogenic differentiation of MSCs, increase fibronectin binding onto the scaffold surface, and enhance COL I synthesis as well as mineralization of the cultured MSCs in vitro.[47–49]

β1 integrin immunofluorescence analysis

Immunofluorescence studies were conducted to investigate the role of β1 integrin molecules in cell response to the developed membranes (Figure 9). Being a link between the ECM and cytoskeleton proteins, β1 integrin facilitates the attachment of cells onto the biomaterial surface via surface topography as well as bioactive molecules by mediating the interaction between cells and adsorbed matrix proteins from biomimetic environment.[50]

Our results demonstrated that the distribution of β1 integrin was almost identical to that of the actin cytoskeleton, and the high expression of β1 integrin observed in all groups at

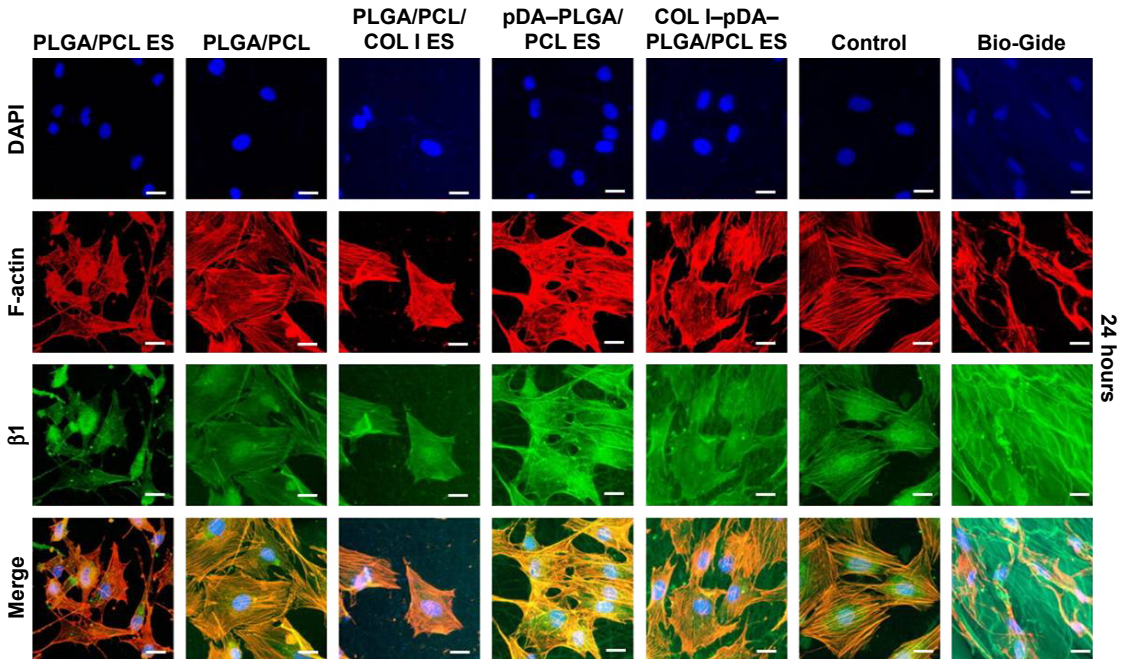

Figure 9 Localization of β1 integrin and F-actin protein was identified by immunofluorescence staining at 24 hours after seeding on five different membranes compared with untreated coverslips (control) and Bio-Gide Collagen membranes (PLGA/PCL ES; PLGA/PCL; PLGA/PCL/COL I ES; pDA–PLGA/PCL ES; COL I–pDA–PLGA/PCL ES).
Notes: Cells were observed by CLSM (×400) and immunostained for F-actin (red), nucleus (blue), and β1 (green). The bottom rows in each panel show the merged images. Control, untreated coverslips; Bio-Gide, collagen membranes. Scale bars =20 μm.
Abbreviations: PLGA, poly(lactic-co-glycolic acid); PCL, poly(caprolactone); ES, electrospinning; COL I, collagen I; pDA, 3,4-dihydroxyphenylalanine; CLSM, confocal laser scanning microscopy; DAPI, 4′,6-diamidino-2-phenylindole.

24 hours. While cultured in the 3D nanofiber membranes, cells attached, stretched, and grew with discrete filopodia along the axis of the nanofiber showing a 3D distribution of the nuclei and the cytoskeleton. Being collected at a random orientation by ES, the axes of the nanofibers were multidirectional. So, the multidirectional distribution of the nuclei and the cytoskeleton was well demonstrated in the CLSM results in such a 3D culturing environment. Distinct from the 2D distribution of the cells cultured in the flat membrane (eg, the solvent-casted PLGA/PCL membrane and Bio-Gide Collagen membrane) or surface (untreated coverslips), the 3D distribution of the cells cultured in the ES membrane recruited much more cells in the same area. Then, the cells infiltrated, grew along the 3D nanofibers, and generated xenogenic (noe)-ECM for another cascade of cell adhesion, differentiation, and mineralization by upregulating cell surface interactions to initiate this cascade. These indicated that besides the effect of surface topography and bioactive molecules on adhesion, the 3D biomimetic architecture of the ES membranes may also provide an advantage in cell adhesion and spreading, which is consistent with the CLSM results.

RT-PCR analyses of β1 integrin expression

We have known that integrins can facilitate cell attachment and spreading as well as regulate intracellular signaling by acting as a bridge between the cell and ECM proteins. Figure 10 shows the mRNA expression level of β1 integrin analyzed by RT-PCR to investigate the various adhesion receptors during the adhesion process. The mRNA expression level of the β1 integrin in COL I–pDA–PLGA/PCL ES membranes was obviously upregulated than the other groups when cells were seeded for 12 hours ($P<0.05$). At 24 hours after seeding, mRNA expression of β1 integrin in pDA–PLGA/PCL ES and COL I–pDA–PLGA/PCL ES membranes was found to be increased compared to the control group ($P<0.05$). The β1 integrin mRNA expression level was found to be upregulated in the PLGA/PCL, PLGA/PCL ES, PLGA/PCL–COL I ES, pDA–PLGA/PCL ES, and the COL I–pDA–PLGA/PCL ES membranes in comparison with the control ($P<0.05$) after seeding for 48 hours. The pDA–PLGA/PCL ES and the COL I–pDA–PLGA/PCL ES membranes showed relatively higher mRNA expression level in β1 integrin than the others. The results indicate that the topography and bioactive properties are linked with the β1 integrin mRNA expression of cells and the combination of these two characteristics can contribute to an enhanced effect. β1 integrin protein expression in the cells grown on pDA was significantly higher than cells grown on other membranes, suggesting that rough topography and the bioactive characteristics play an important role in cell adhesion.

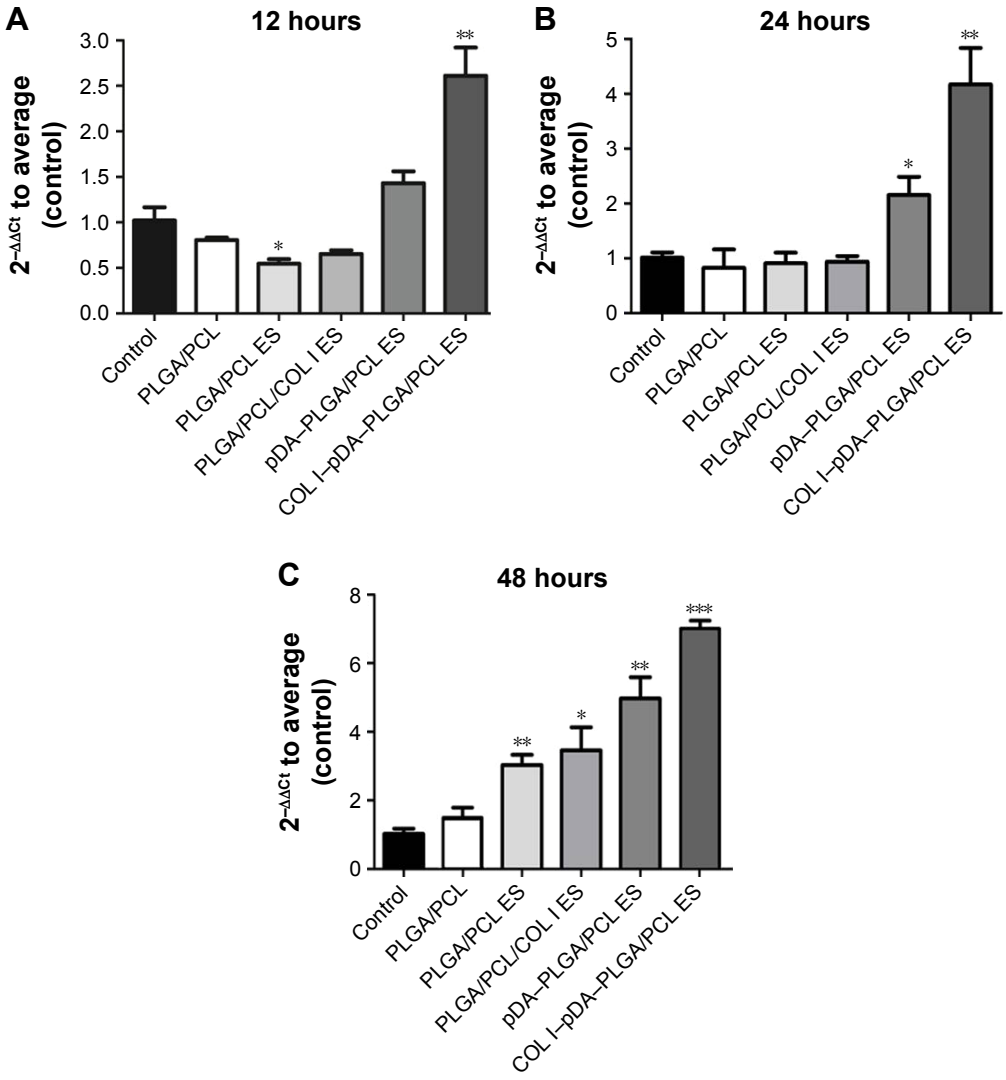

Figure 10 Gene expression level of β1 integrin relative to GAPDH in cells cultured on the surfaces of PLGA/PCL, PLGA/PCL ES, PLGA/PCL/COL I ES, pDA–PLGA/PCL ES, COL I–pDA–PLGA/PCL ES, and the untreated coverslips (blank control), at 12 (**A**), 24 (**B**), and 48 (**C**) hours.
Notes: *$P<0.05$ vs control. **$P<0.01$ vs control. ***$P<0.001$ vs control.
Abbreviations: GAPDH, glyceraldehyde-3-phosphate dehydrogenase; PLGA, poly(lactic-co-glycolic acid); PCL, poly(caprolactone); ES, electrospinning; COL I, collagen I; pDA, 3,4-dihydroxyphenylalanine.

In osteogenic differentiation and mineralization of preosteoblasts, collagen synthesis precedes the expression of osteogenic markers indicating that the interaction of ECM components with the integrin family of cell surface receptors plays a role in the induction of osteogenesis.[24] Xiao et al observed that disruption of the α_2 integrin–ECM interactions with antibodies or peptides specific to the cell-binding domain of collagen type I abolished the expression of osteocalcin mRNA and mineralization in MC3T3-E1 cells, indicating that integrin-binding ligands, as part of the ECM components, are required for induction of osteoblast-specific gene expression.[51] Conjugation reactions have been used to covalently attach osteogenic proteins/peptides to the biomaterials, thus prolonging their residence time.[52] For example, grafting the osteogenic protein/peptide to the surface of nanoparticles not only immobilizes and slowly releases the bioactive agent with time but also presents a multivalent form of the protein/peptide for stronger interaction with cell surface receptors, leading to a more intense activation of osteogenic signaling pathways.[53] In our study, an alternative approach is to covalently graft COL I to the surface of nanofiber ES membranes assisted by pDA coating. Moreover, pDA–PLGA/PCL ES supported high degree of cell adhesion and proliferation. More importantly, the results showed that the surface of COL I–pDA–PLGA/PCL ES membranes exposed more collagen active sites than the surface of PLGA/PCL/COL I ES with the same amount of COL I in bulk phase. Higher expression of β1 integrin was detected in COL I-related groups such

as COL I–pDA–PLGA/PCL ES and Bio-Gide Collagen membranes. It demonstrated that combining mussel-spirited method and ES could provide a novel platform technology to develop tunable, functional, biocompatible, 3D scaffolds for bone repairing.[54]

Conclusion

In this work, PLGA/PCL membranes with both biomimetic architecture and bioactive surface were constructed by ES and mussel-spirited method. Strikingly, the COL I was attached to the 3D nanofibrous membranes by blending and pDA-mediated modification. It was demonstrated that the functionalized PLGA/PCL membranes were noncytotoxic and exhibited better biocompatibility. The cell adhesion, proliferation, and osteodifferentiation of cultured MC3T3-E1 in vitro could be significantly elevated by synergistic effects of the 3D nanofibrous architecture and COL I. While cultured in the 3D nanofiber membranes, cells attached, stretched, and grew with discrete filopodia along the axis of the nanofiber, and showed a 3D distribution of the nuclei and the cytoskeleton. The surface of COL I–pDA–PLGA/PCL ES membranes exposed more collagen active sites that enhanced the preosteoblast response. Therefore, the results demonstrated that further improvement in the GBR technique can be achieved by using such modified PLGA/PCL electrospun membranes. Those membranes open new pathway for proliferating MC3T3-E1 cells in a 3D pattern, and bring in broad spectrum of possibilities to accelerate the biological guidance for bone formation.

Acknowledgments

This work was supported by the National Key Research and Development Plan (2016YFA0201704), National Nature Science Foundation of China (numbers 31200757 and 21501027), Medical Leading Personnel and Innovation Team of Jiangsu Province (zcb2012016), Priority Academic Program Development of Jiangsu Higher Education Institutions (2014-37), Suzhou Health and Family Planning Commission (SYSD2015093), and Collaborative Innovation Center of Suzhou Nano Science and Technology. The authors would like to express their gratitude to Xingshun Xu (professor of the Second Affiliated Hospital of Soochow University, People's Republic of China) for providing technical support of CLSM, and Yuting Zhu, Ju Yin, and Danyun Liu (students in Southeast University Chengxian College, People's Republic of China) for exploring ES parameters of polymeric membranes.

Disclosure

The authors report no conflicts of interest in this work.

References

1. Blanco J, Alonso A, Sanz M. Long-term results and survival rate of implants treated with guided bone regeneration: a 5-year case series prospective study. *Clin Oral Implants Res*. 2005;16(3):294–301.
2. Venkatesan J, Bhatnagar I, Manivasagan P, Kang KH, Kim SK. Alginate composites for bone tissue engineering: a review. *Int J Biol Macromol*. 2015;72:269–281.
3. Beitlitum I, Artzi Z, Nemcovsky CE. Clinical evaluation of particulate allogeneic with and without autogenous bone grafts and resorbable collagen membranes for bone augmentation of atrophic alveolar ridges. *Clin Oral Implants Res*. 2010;21(11):1242–1250.
4. Bottino MC, Thomas V, Schmidt G, et al. Recent advances in the development of GTR/GBR membranes for periodontal regeneration-a materials perspective. *Dent Mater*. 2012;28(7):703–721.
5. Gentile P, Chiono V, Tonda-Turo C, Ferreira AM, Ciardelli G. Polymeric membranes for guided bone regeneration. *Biotechnol J*. 2011;6(10):1187–1197.
6. Tolba E, Muller WEG, El-Hady BMA, et al. High biocompatibility and improved osteogenic potential of amorphous calcium carbonate/vaterite. *J Mater Chem B*. 2016;4(3):376–386.
7. Behring J, Junker R, Walboomers XF, Chessnut B, Jansen JA. Toward guided tissue and bone regeneration: morphology, attachment, proliferation, and migration of cells cultured on collagen barrier membranes. A systematic review. *Odontology*. 2008;96(1):1–11.
8. Quinlan E, Lopez-Noriega A, Thompson E, Kelly HM, Cryan SA, O'Brien FJ. Development of collagen-hydroxyapatite scaffolds incorporating PLGA and alginate microparticles for the controlled delivery of rhBMP-2 for bone tissue engineering. *J Control Release*. 2015;198:71–79.
9. Shim JH, Huh JB, Park JY, et al. Fabrication of blended polycaprolactone/poly(lactic-co-glycolic acid)/beta-tricalcium phosphate thin membrane using solid freeform fabrication technology for guided bone regeneration. *Tissue Eng Part A*. 2013;19(3–4):317–328.
10. Yang HS, Park J, La WG, Jang HK, Lee M, Kim BS. 3,4-Dihydroxyphenylalanine-assisted hydroxyapatite nanoparticle coating on polymer scaffolds for efficient osteoconduction. *Tissue Eng C*. 2012;18(4):245–251.
11. Li WJ, Cooper JA, Mauck RL, Tuan RS. Fabrication and characterization of six electrospun poly(alpha-hydroxy ester)-based fibrous scaffolds for tissue engineering applications. *Acta Biomater*. 2006;2(4):377–385.
12. La WG, Jang J, Kim BS, Lee MS, Cho DW, Yang HS. Systemically replicated organic and inorganic bony microenvironment for new bone formation generated by a 3D printing technology. *RSC Adv*. 2016;6(14):11546–11553.
13. Li XR, Xie JW, Yuan XY, Xia YN. Coating electrospun poly(epsilon-caprolactone) fibers with gelatin and calcium phosphate and their use as biomimetic scaffolds for bone tissue engineering. *Langmuir*. 2008;24(24):14145–14150.
14. Katsanevakis E, Wen XJ, Zhang N. Creating electrospun nanofiber-based biomimetic scaffolds for bone regeneration. In: Jayakumar R, Nair SV, editors. *Biomedical Applications of Polymeric Nanofibers*. Vol 246. Berlin: Springer-Verlag Berlin; 2012:63–100.
15. Hutmacher DW. Scaffold design and fabrication technologies for engineering tissues – state of the art and future perspectives. *J Biomater Sci Polym Ed*. 2001;12(1):107–124.
16. Liao S, Watari F, Zhu Y, et al. The degradation of the three layered nano-carbonated hydroxyapatite/collagen/PLGA composite membrane in vitro. *Dent Mater*. 2007;23(9):1120–1128.
17. Wang T, Yang XY, Qi X, Jiang CY. Osteoinduction and proliferation of bone-marrow stromal cells in three-dimensional poly (epsilon-caprolactone)/hydroxyapatite/collagen scaffolds. *J Transl Med*. 2015;13:11.
18. Bottino MC, Thomas V, Janowski GM. A novel spatially designed and functionally graded electrospun membrane for periodontal regeneration. *Acta Biomater*. 2011;7(1):216–224.
19. Li JS, Li Y, Liu X, Zhang J, Zhang Y. Strategy to introduce an hydroxyapatite-keratin nanocomposite into a fibrous membrane for bone tissue engineering. *J Mater Chem B*. 2013;1(4):432–437.

20. Wang JB, Wu DY, Zhang ZZ, et al. Biomimetically ornamented rapid prototyping fabrication of an apatite-collagen-polycaprolactone composite construct with nano-micro-macro hierarchical structure for large bone defect treatment. *ACS Appl Mater Interfaces*. 2015;7(47):26244–26256.
21. Ji W, Yang F, Ma JL, et al. Incorporation of stromal cell-derived factor-1 alpha in PCL/gelatin electrospun membranes for guided bone regeneration. *Biomaterials*. 2013;34(3):735–745.
22. Chen G, Xia Y, Lu XL, Zhou XF, Zhang FM, Gu N. Effects of surface functionalization of PLGA membranes for guided bone regeneration on proliferation and behavior of osteoblasts. *J Biomed Mater A*. 2013;101(1):44–53.
23. Kim SE, Yun YP, Shim KS, et al. Fabrication of a BMP-2-immobilized porous microsphere modified by heparin for bone tissue engineering. *Colloids Surface B Interfaces*. 2015;134:453–460.
24. Jabbari E. Osteogenic peptides in bone regeneration. *Curr Pharm Des*. 2013;19(19):3391–3402.
25. McMahon RE, Wang LN, Skoracki R, Mathur AB. Development of nanomaterials for bone repair and regeneration. *J Biomed Mater Res B*. 2013;101B(2):387–397.
26. Masters KS. Covalent growth factor immobilization strategies for tissue repair and regeneration. *Macromol Biosci*. 2011;11(9):1149–1163.
27. Kiran S, Nune KC, Misra RDK. The significance of grafting collagen on polycaprolactone composite scaffolds: processing-structure-functional property relationship. *J Biomed Mater A*. 2015;103(9):2919–2931.
28. Kleinman HK, Klebe RJ, Martin GR. Role of collagenous matrices in the adhesion and growth of cells. *J Cell Biol*. 1981;88(3):473–485.
29. Wang LM, Stegemann JP. Glyoxal crosslinking of cell-seeded chitosan/collagen hydrogels for bone regeneration. *Acta Biomater*. 2011;7(6):2410–2417.
30. Ito Y, Liu SQ, Imanishi Y. Enhancement of cell-growth on growth factor-immobilized polymer film. *Biomaterials*. 1991;12(5):449–453.
31. Ko E, Yang K, Shin J, Cho SW. Polydopamine-assisted osteoinductive peptide immobilization of polymer scaffolds for enhanced bone regeneration by human adipose-derived stem cells. *Biomacromolecules*. 2013;14(9):3202–3213.
32. Ruder C, Sauter T, Kratz K, et al. Influence of fibre diameter and orientation of electrospun copolyetheresterurethanes on smooth muscle and endothelial cell behaviour. *Clin Hemorheol Microcirc*. 2013;55(4):513–522.
33. Seo CH, Furukawa K, Montagne K, Jeong H, Ushida T. The effect of substrate microtopography on focal adhesion maturation and actin organization via the RhoA/ROCK pathway. *Biomaterials*. 2011;32(36):9568–9575.
34. Teo BKK, Ankam S, Chan LY, Yim EKF. Nanotopography/mechanical induction of stem-cell differentiation. In: Shivashankar GV, editor. *Nuclear Mechanics and Genome Regulation*. Vol 98. San Diego, CA: Elsevier Academic Press Inc; 2010:241–294.
35. Tarone G, Hirsch E, Brancaccio M, et al. Integrin function and regulation in development. *Int J Dev Biol*. 2000;44(6):725–731.
36. Kanchanawong P, Shtengel G, Pasapera AM, et al. Nanoscale architecture of integrin-based cell adhesions. *Nature*. 2010;468(7323):580–584.
37. Jing X, Mi HY, Wang XC, Peng XF, Turng LS. Shish-Kebab-structured poly(epsilon-caprolactone) nanofibers hierarchically decorated with chitosan poly(epsilon-caprolactone) copolymers for bone tissue engineering. *ACS Appl Mater Interfaces*. 2015;7(12):6955–6965.
38. Jia J, Liu G, Guo ZX, Yu J, Duan YY. Preparation and characterization of soluble eggshell membrane protein/PLGA electrospun nanofibers for guided tissue regeneration membrane. *J Nanometer*. 2012;2012:282736.
39. Chen JP, Chang YS. Preparation and characterization of composite nanofibers of polycaprolactone and nanohydroxyapatite for osteogenic differentiation of mesenchymal stem cells. *Colloids Surface B Interfaces*. 2011;86(1):169–175.
40. Wang JH, Yang Q, Cheng NM, et al. Collagen/silk fibroin composite scaffold incorporated with PLGA microsphere for cartilage repair. *Mater Sci Eng C Mater Biol Appl*. 2016;61:705–711.
41. Yang K, Lee JS, Kim J, et al. Polydopamine-mediated surface modification of scaffold materials for human neural stem cell engineering. *Biomaterials*. 2012;33(32):8186–8187.
42. Lee YB, Shin YM, Lee JH, et al. Polydopamine-mediated immobilization of multiple bioactive molecules for the development of functional vascular graft materials. *Biomaterials*. 2012;33(33):8343–8352.
43. Prabhakaran MP, Mobarakeh LG, Kai D, Karbalaie K, Nasr-Esfahani MH, Ramakrishna S. Differentiation of embryonic stem cells to cardiomyocytes on electrospun nanofibrous substrates. *J Biomed Mater Res B*. 2014;102(3):447–454.
44. Tillman BW, Yazdani SK, Lee SJ, Geary RL, Atala A, Yoo JJ. The in vivo stability of electrospun polycaprolactone-collagen scaffolds in vascular reconstruction. *Biomaterials*. 2009;30(4):583–588.
45. Bosetti M, Fusaro L, Nicoli E, Borrone A, Aprile S, Cannas M. Poly-L-lactide acid-modified scaffolds for osteoinduction and osteoconduction. *J Biomed Mater A*. 2014;102(10):3531–3539.
46. Li N, Chen G, Liu J, et al. Effect of surface topography and bioactive properties on early adhesion and growth behavior of mouse preosteoblast MC3T3-E1 cells. *ACS Appl Mater Interfaces*. 2014;6(19):17134–17143.
47. DeVolder RJ, Kim IW, Kim ES, Kong H. Modulating the rigidity and mineralization of collagen gels using poly(lactic-co-glycolic acid) microparticles. *Tissue Eng Part A*. 2012;18(15–16):1642–1651.
48. Jiang YZ, Chen LK, Zhang SF, et al. Incorporation of bioactive polyvinylpyrrolidone-iodine within bilayered collagen scaffolds enhances the differentiation and subchondral osteogenesis of mesenchymal stem cells. *Acta Biomater*. 2013;9(9):8089–8098.
49. Faia-Torres AB, Goren T, Ihalainen TO, et al. Regulation of human mesenchymal stem cell osteogenesis by specific surface density of fibronectin: a gradient study. *ACS Appl Mater Interfaces*. 2015;7(4):2367–2375.
50. Gandavarapu NR, Mariner PD, Schwartz MP, Anseth KS. Extracellular matrix protein adsorption to phosphate-functionalized gels from serum promotes osteogenic differentiation of human mesenchymal stem cells. *Acta Biomater*. 2013;9(1):4525–4534.
51. Xiao GZ, Wang D, Benson MD, Karsenty G, Franceschi RT. Role of the alpha(2)-integrin in osteoblast-specific gene expression and activation of the Osf2 transcription factor. *J Biol Chem*. 1998;273(49):32988–32994.
52. He XZ, Yang XM, Jabbari E. Combined effect of osteopontin and BMP-2 derived peptides grafted to an adhesive hydrogel on osteogenic and vasculogenic differentiation of marrow stromal cells. *Langmuir*. 2012;28(12):5387–5397.
53. Mercado AE, Yang XM, He XZ, Jabbari E. Effect of grafting BMP2-derived peptide to nanoparticles on osteogenic and vasculogenic expression of stromal cells. *J Tissue Eng Regen Med*. 2014;8(1):15–28.
54. Wu X, Wang S. Regulating MC3T3-E1 cells on deformable poly(ε-caprolactone) honeycomb films prepared using a surfactant-free breath figure method in a water-miscible solvent. *ACS Appl Mater Interfaces*. 2012;4(9):4966–4975.